Journal of Physics: Conference Series

PAPER • **OPEN ACCESS**

CFD simulation of a 2 bladed multi megawatt wind turbine with flexible rotor connection

To cite this article: L Klein *et al* 2016 *J. Phys.: Conf. Ser.* **753** 022010

CFD simulation of a 2 bladed multi megawatt wind turbine with flexible rotor connection

L Klein[1], B Luhmann[2], K-N Rösch[1], T Lutz[1], P-W Cheng[2] and E Krämer[1]

[1]Institute of Aerodynamics und Gas Dynamics (IAG), University of Stuttgart, Pfaffenwaldring 21, 70569 Stuttgart, Germany
[2]Stuttgart Wind Energy (SWE) @ Institute of Aircraft Design, University of Stuttgart, Allmandring 5b, 70569 Stuttgart, Germany

levin.klein@iag.uni-stuttgart.de

Abstract. An innovative passive load reduction concept for a two bladed 3.4 MW wind turbine is investigated by a conjoint CFD and MBS - BEM methodology. The concept consists of a flexible hub mount which allows a tumbling motion of the rotor. First, the system is simulated with a MBS tool coupled to a BEM code. Then, the resulting motion of the rotor is extracted from the simulation and applied on the CFD simulation as prescribed motion. The aerodynamic results show a significant load reduction on the support structure. Hub pitching and yawing moment amplitudes are reduced by more than 50% in a vertically sheared inflow. Furthermore, the suitability of the MBS – BEM approach for the simulation of the load reduction system is shown.

1. Introduction

Two bladed multi megawatt wind turbines are considered to have a high potential in reducing the cost of energy compared to three bladed turbines [1]. The Skywind 3.4 MW turbine combines several concepts to achieve this goal. From an integrated lift system for crane-less rotor installation to a hybrid concrete-steel tower. To overcome the higher unsteady loads of two bladed turbines, the potential of an innovative passive load reduction system is investigated. For installation purposes, the nacelle of the turbine is split into a front part, the hub mount, and a rear part, the turbine mount. By applying flexibility to the connection in-between the two parts, this feature gives the opportunity to add two additional degrees of freedom (pitch and yaw) to the rotor which allows small tumbling excursions of the whole rotor (Figure 1).

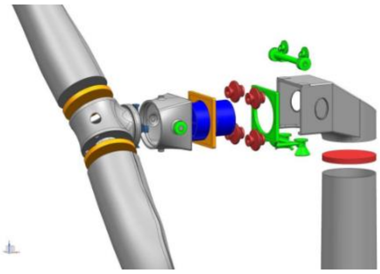

Figure 1. Schematic view of the turbine with the flexible connection for the passive load reduction concept (courtesy of Skywind GmbH).

2. Approach

The load reduction system is investigated numerically using CFD (Computational Fluid Dynamics) and a MBS (Multibody Simulation) solver coupled to a BEM (Blade Element Momentum) code. For the simulations the flexibility has been approximated by a Cardan joint with two degrees of freedom. The general approach is to adjust the stiffness of the flexible connection between hub mount and turbine mount with the MBS to obtain an optimal load reduction within the given restrictions for the excursions. The tumbling motion of the rotor is then extracted from the results and introduced into the CFD simulation as prescribed motion to validate the results of the MBS and to gain further insight into the aerodynamics.

The simulations are conducted with sheared inflow using a steady logarithmic wind profile with a surface roughness of 0.59 and rated wind speed of 11.4 m/s at hub height. To maintain comparability, the rotational frequency is fixed at 17 rpm and the constant pitch angle has been set consistent to the provided power curve. Furthermore, as fluid structure coupling could not be considered in CFD (e.g. blade flexibility), all structures are rigid in CFD as well as in MBS.

2.1. MBS

The excursions of the flexible hub connection are obtained using the coupled multibody simulation code Simpack. Aerodynamic forces in the deterministic sheared inflow are calculated by the BEM approach inherited in ECN's AeroModule. The aerodynamic approach has been verified for load inducing operational conditions on two bladed wind turbines by comparing the BEM approach to a more advanced lifting-line method [2]. The hub degree of freedom is modelled as a Cardan joint between the turbine mount and the hub mount. The position of the center of rotation of the Cardan joint is displayed in Figure 2.

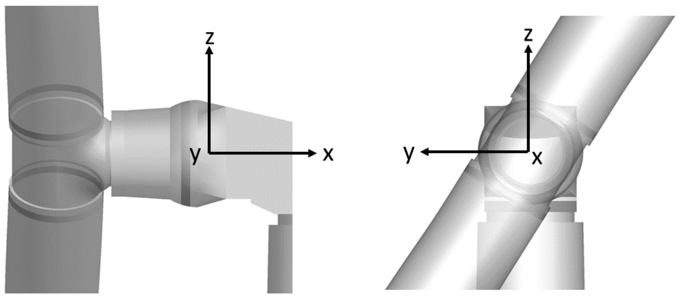

Figure 2. Turbine in side and front view. Position of the center of rotation of the Cardan joint and definition of the coordinate system. X-axis is rotor axis. Cardan joint allows rotation around y-axis and z-axis.

A uniform, rotational spring-damper element is applied to mitigate the excursion displacements and velocities. The spring-damper is parameterized such that excursions are limited to the design boundaries, yet aerodynamically induced excitations are significantly reduced. From these BEM coupled simulations it is observed that fatigue life can be increased by a combination of structural decoupling and a reduction of the aerodynamic fluctuations at the blades [3]. The 2P periodic excursions are extracted to serve as input for the CFD simulation.

2.2. CFD

The block-structured finite volume solver FLOWer [4] is applied for the CFD simulation of the turbine. FLOWer has been used and extended for several years in fields of wind energy at IAG [5][6][7]. All simulations for this study are carried out fully turbulent with the second order spatial discretization scheme JST and a dual time stepping scheme for discretization in time. The Menter SST model is applied for turbulence modelling. Due to the implemented Chimera technique [8] individually adapted grids for all structures can be realized, as well as relative motion between grids. The time step has been set correspondingly to an azimuthal step of 2°. A grid convergence study according to Celik [9] has been

carried out in previous work using a one half model of the turbine with periodic boundary conditions to determine the grid dependency of the solution [10].
The CFD setup consists of seven individual grids. The six grids, discretizing the surface of the wind turbine, are embedded in a background grid. On all surfaces the boundary layer is fully resolved. Hanging grid node technique is used for the background grid, as it enables cost efficient refinement. Figure 3 and Figure 4 show longitudinal cuts through the CFD domain with the rotor in vertical position. The refinement with hanging grid nodes in the background grid as well as the overlapping grids can be seen.

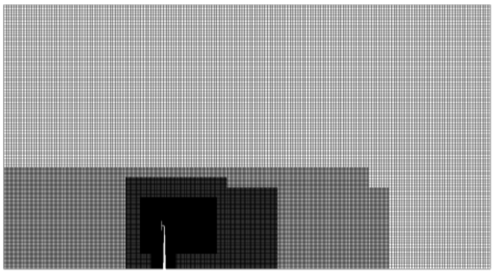

Figure 3. Longitudinal cut through the whole CFD domain at turbine position.

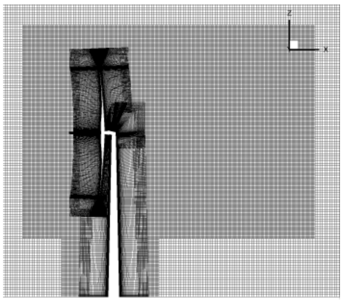

Figure 4. Longitudinal cut through the CFD domain at turbine position (detail of Figure 3).

The easiest way to enable a tumbling motion of the rotor in the CFD simulation is to exclude nacelle and tower and simulate the rotor only. As the influence of the tower blockage cannot be considered then, a more complex simulation set-up, including nacelle and tower, was chosen. To enable a tumbling motion of the rotor, the nacelle grid has been split into a fixed rear part and a moving front part. As the flexibility is modelled as Cardan joint, the center of rotation is fixed. A sphere has been inserted into the nacelle geometry where the two grids overlap on the surface without violating the geometric boundaries when the rotor tumbles as they are sliding on the surface of the sphere (Figure 5 and Figure 6).

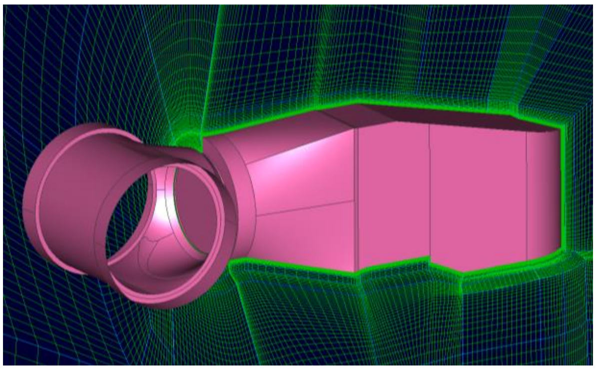

Figure 5. Original nacelle surface and grid.

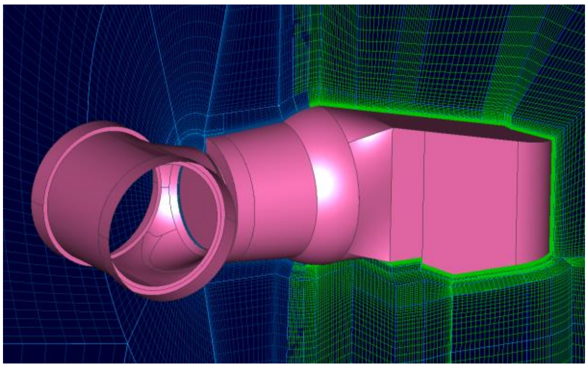

Figure 6. Adopted nacelle surface and grid with sphere surface for sliding of overlapping grids.

The excursions extracted from the Simpack simulation, represented by two Euler angles around the z-axis (γ) and the rotated y-axis (β) have been analyzed by FFT (Fast Fourier Transformation) and approximated by Fourier series. The position of the center of rotation and the definition of the coordinate system can be found in Figure 2.
To achieve convergence of the loads and to have aerodynamic loads for comparison, the turbine is simulated for 26 revolution without rotor motion first (rigid). Polynomials have been defined for the transition from rigid rotor to flexible rotor motion to avoid discontinuous motion and unrealistic aerodynamic loads. The polynomials are applied for half a revolution. Then the excursions of the rotor

are applied on the CFD grid by Fourier series for five revolutions. In Figure 7 the extracted data from Simpack are shown together with the polynomials and Fourier curves. As far as one can see, the motion can be approximated adequately with the chosen 7th order Fourier series.

Figure 8 shows the relative x-position and the x-velocity of the blade tip in the global coordinate system. Positive velocities indicate a downwind motion and negative velocities an upwind motion of the blade tip. This means that between 50° and 230° azimuth the blade is advancing the wind which results in an augmentation of the local angle of attack. The local angle of attack (AoA) is also directly influenced by γ and β. As β is generally higher than 0°, for the down going blade the AoA is reduced and for the up going blade it is increased. As γ is lower 0° at 0° and 180° azimuth, the AoA is reduced around 0° and increased around 180°. Together, both effects should lead to an increase of the local AoA in the lower half of the rotor and to a decrease in the upper half. This should directly correspond to an according change of lift and therefore of thrust for one blade. A shift of the blade thrust force curve towards the lower side of the rotor can be expected.

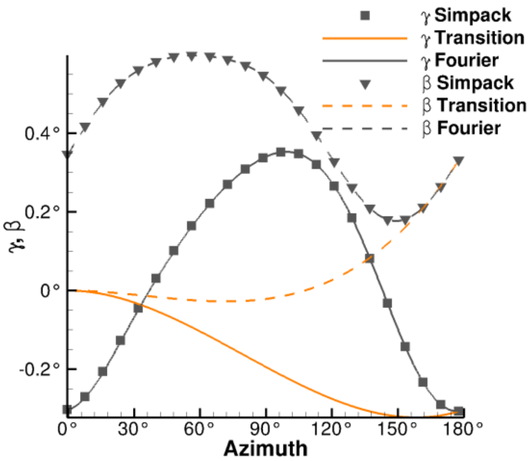

Figure 7. Tumbling motion of the rotor. Extracted data from Simpack and prescribed motion of the rotor in FLOWer. γ represents the angle around the z-axis and β the angle around the rotated y-axis. Signal is 2P periodic and one period is displayed. The motion is approximated by a Fourier series and the smooth transition from rigid into the Fourier series is realized by polynomials.

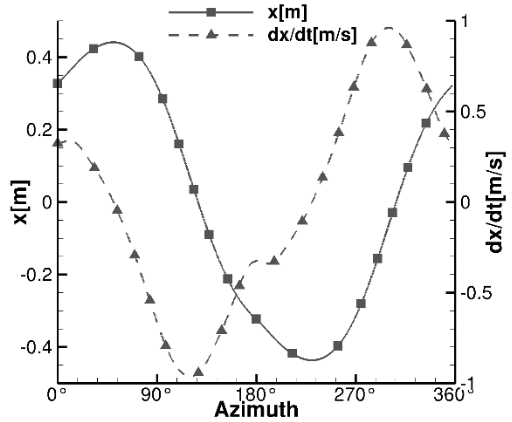

Figure 8. Blade tip position in global x direction and x-velocity of blade tip (dx/dt) caused by the tumbling motion of the rotor.

3. Results

To analyze the effect of the passive load reduction system on the aerodynamic loads of the CFD results, the aerodynamic forces and moments are evaluated in the non-rotating hub coordinate system with the x-axis equal the rotor axis. Its origin is located in the center of the hub and thus tumbles with the rotor. In the rigid state, the y-axis is horizontal and the z-axis vertically upright. The highest loads fluctuations on the rotor occur in the moments M_y and M_z which are displayed in Figure 9 and Figure 10 for overall 10.5 revolutions (5 rigid, 0.5 transition, 5 flexible) with respect to the azimuth angle of the first blade. 0° corresponds to upright position. They are normalized using the average load of the rigid simulation. To quantify the magnitude of the moments, their relation to Torque (M_x) in the rigid case is listed below:

$$\frac{M_{y_{max}}}{M_{x_{max}}} = 0.61 \qquad \frac{M_{z_{max}}}{M_{x_{max}}} = 0.24 \tag{1}$$

Both loads are dominated by the vertically sheared inflow. While M_y is highest in upright position where the velocity difference between the two blades and the lever arm are highest, the minimum M_y occurs in horizontal position. The moment around the z-axis (M_z) is oscillating with high amplitude compared to the average value. In vertical and horizontal position of the rotor M_z crosses zero. The maximum is reached at approx. 45° and the minimum at approx. 135° of the downwards running blade. For both loads the prescribed hub motion leads to a strong reduction of the mean values as well as the amplitudes. M_y is reduced by more than 50% in the amplitude. For M_z, the amplitude is reduced even more, shifting the mean moment to negative values.

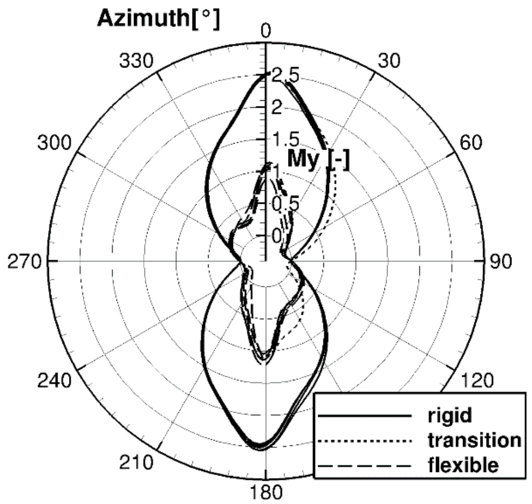

Figure 9. CFD: Normalized aerodynamic moment around the non-rotating rotor y-axis (pitch).

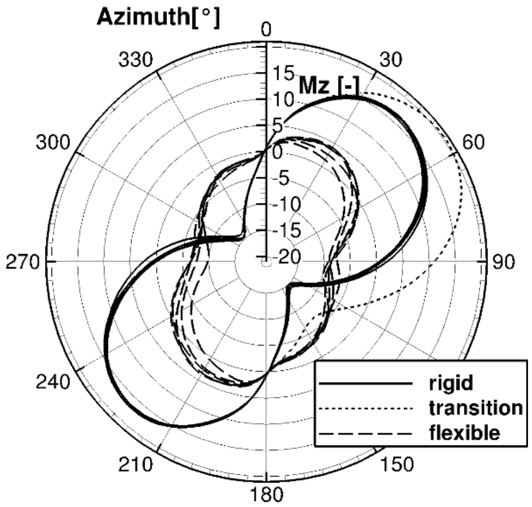

Figure 10. CFD: Normalized aerodynamic moment around the non-rotating rotor z-axis (yaw).

Although load reduction is obvious, the normalized loads of the rigid and flexible case have been analyzed by means of FFT. The frequency has been normalized using the rotational frequency of the turbine. The results are shown in Figure 11 and Figure 12. The main peaks are visible for the 2P frequency and its higher harmonics, as for the investigated case the significant influences (vertically sheared inflow and tower blockage) act in this frequency. Consequently, for both, M_y and M_z, the highest amplitude occurs at the 2P frequency. This 2P amplitude is reduced by approx. 65% for M_y as well as M_z in the flexible case. For some other frequencies (e.g. 1P) the amplitudes slightly increase, but the magnitudes are significantly lower than the 2P amplitude.

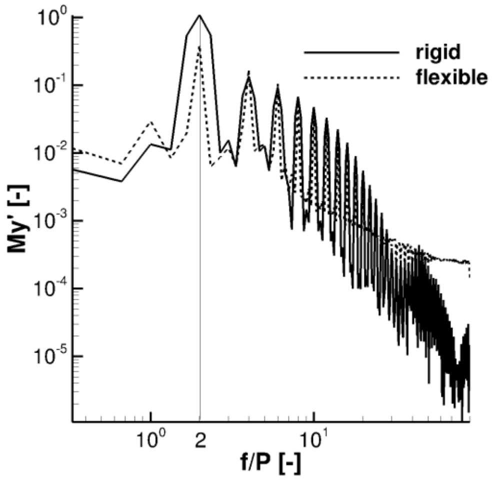

Figure 11. CFD: Result of the FFT analyses, amplitude of the normalized aerodynamic moment around the rotor fixed non-rotating y-axis (pitch).

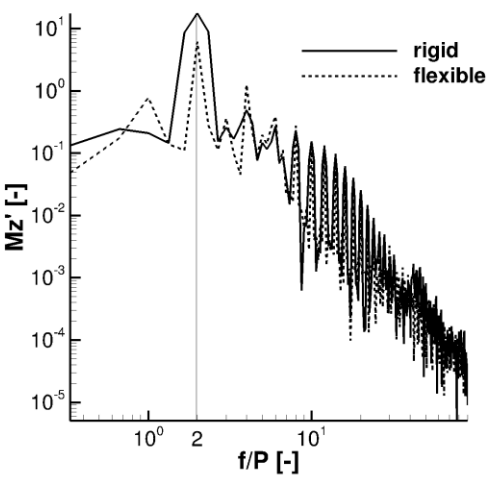

Figure 12. CFD: Result of the FFT analyses, amplitude of the normalized aerodynamic moment around the rotor fixed non-rotating z-axis (yaw).

Torque (M_x) and thrust (F_x) of the rotor are almost not influenced by the tumbling motion of the rotor, while a load reduction for all forces and moments can be observed for the individual blades. Normalized thrust and torque for one blade are displayed in Figure 13 and Figure 14. For both loads the 1P amplitudes are reduced by more than 60% compared to the rigid case. The tumbling motion of the rotor leads to a shift of these loads to the lower left side of the diagram and results in a shift of the maxima to the 270° position. This partly confirms the observations concerning the change in the local angle of attack. Shift to the lower side was expected. Although the blade is moving downwind at the 270° position, thrust is increased. This leads to the conclusion that in this azimuth region the change in AoA by β and γ has a higher influence than the velocity of the blade in x-direction. The influence of the tower blockage at 180° is also reduced, leading to a smoother and less sharp decrease of the loads in front of the tower. As the moments M_y and M_z on the rotor are mainly driven by the thrust force of the blades, the reduction of the amplitude in the thrust force of the blades leads to a reduction of the moments on the rotor.

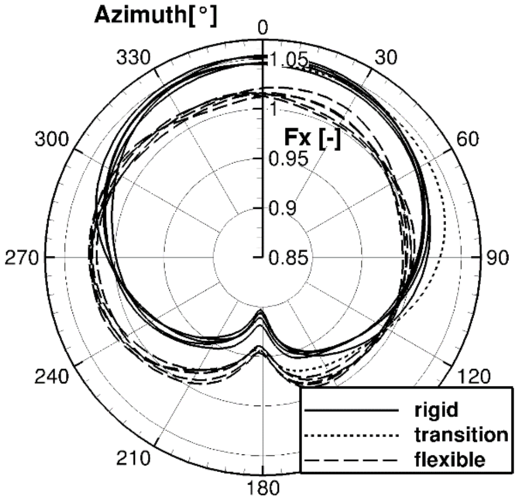

Figure 13. CFD: Normalized aerodynamic thrust force (F_x) for one blade.

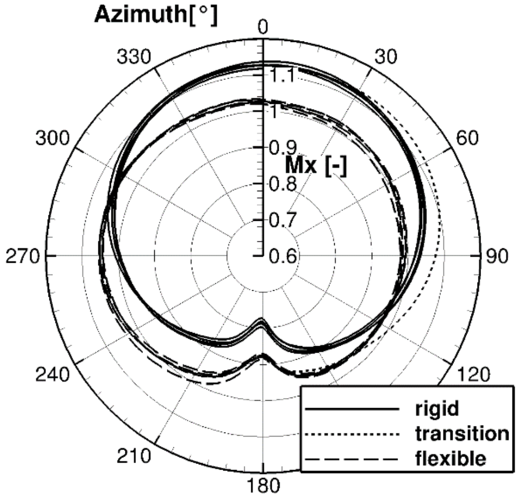

Figure 14. CFD: Normalized aerodynamic torque around the rotor x-axis (M_x) for one blade.

Figure 15 shows the aerodynamic thrust force for one rotor blade for FLOWer and for AeroModule BEM, normalized by the average of the rigid CFD result. In the rigid BEM case the result is shifted to the lower side of the diagram in comparison to the rigid CFD case, with approx. 3% lower load at 0° azimuth. While close to the tower, the loads are almost the same as in CFD, with approx. 1.5% lower loads in front of the tower. In the flexible BEM case the curve is more shifted towards 180° in comparison to the flexible CFD case which is shifted more towards 240°. Compared to the rigid case, the differences at 0° and 180° stay more or less the same, but around 240° they increase and around 120° they decrease. Overall the blade thrust amplitude in BEM is lower compared to CFD for the rigid case as well as for the flexible case. The reasons for this differences in the BEM simulation cannot be clearly detected. The general difference might be a result of the used polars in the BEM calculation that already lead to differences in uniform inflow simulations. But it cannot be validated whether the influence of the rotor motion is considered correctly in the BEM simulation and if there is an influence from this on the shift of the loads.

In Figure 16 the comparison of CFD and BEM for M_y is displayed. In general, the loads are similar for both, the rigid and the flexible case with almost no difference in the position and magnitude of maxima and minima. Thus, the same load reduction as in CFD can be seen in BEM. In detail there are some deviations. CFD is never lower than BEM in the rigid case. Around 160°/340° M_y is approx. 12% lower in BEM and about 15% around 40°/220°. In the flexible case CFD is significantly higher than BEM at 20°/200° and lower at 70°/250° and again significantly higher at 130°/310°. Overall M_y is 7% lower than CFD in the rigid case and 17% lower in the flexible case.

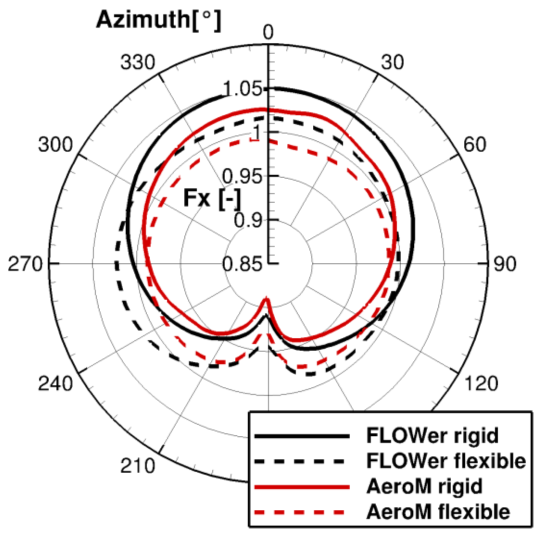

Figure 15. Normalized aerodynamic thrust force (Fx) for one rotor blade. CFD – BEM comparison.

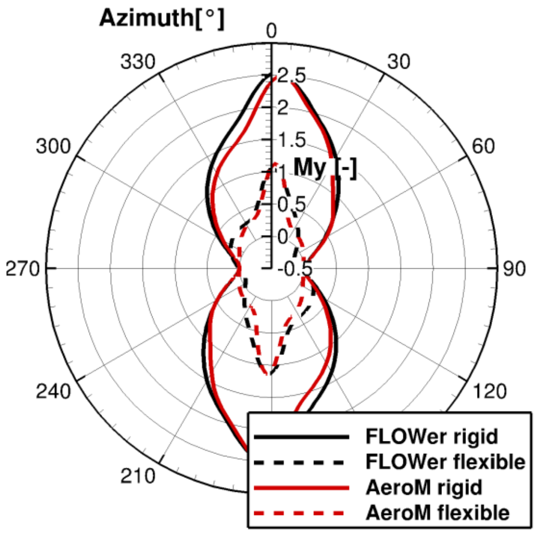

Figure 16. Normalized aerodynamic moment around the non-rotating rotor y-axis (pitch). CFD – BEM comparison.

To quantify the influence of the flexibility on the loads a FFT analyses has been conducted for the BEM results. It has been normalized using the CFD loads of the rigid simulation. The signal of overall 17 revolutions has been used for the FFT. Thus, compared to the CFD results more frequencies can be resolved and the peaks are more distinctive. Figure 17 shows the result for the thrust force F_x of one blade and in Figure 18 the rotor moment M_y is displayed. For M_y, comparable to the CFD result, the peaks are located at the 2P frequency and its higher harmonics while for F_x the peaks are located at the 1P frequency and its higher harmonics. For both loads the first peak is dominant as the magnitude is clearly higher than for higher frequencies. In the flexible case the 1P amplitude of F_x is reduced by 75% and the 2P amplitude of My is reduced by 70%.

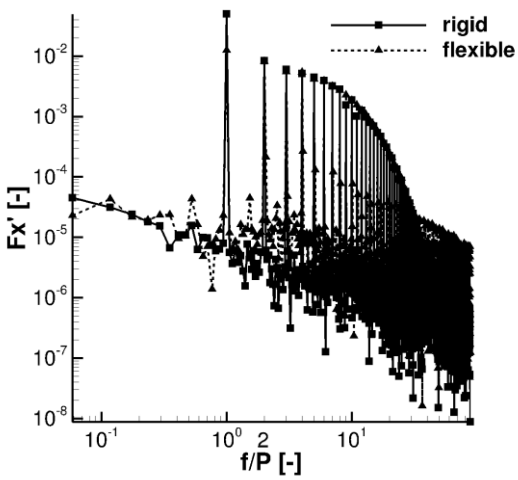

Figure 17. BEM: Result of the FFT analyses, amplitude of the normalized aerodynamic thrust force (F_x) for one rotor blade.

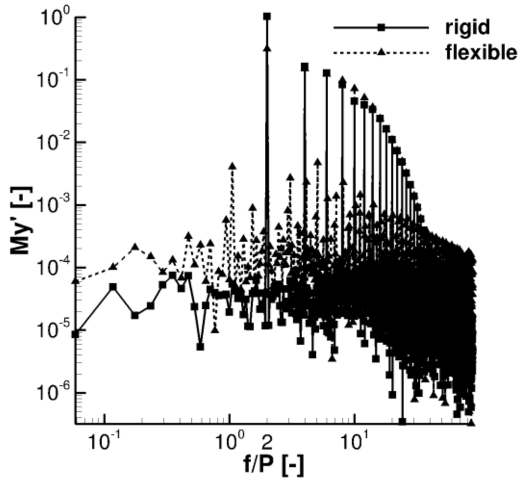

Figure 18. BEM: Result of the FFT analyses, amplitude of the normalized aerodynamic moment around the rotor fixed non-rotating y-axis (pitch).

4. Conclusion

In the present paper an innovative passive load reduction concept on a two bladed 3.4 MW turbine has been investigated using a coupled MBS-BEM method and CFD. The load reduction concept consists of a flexible hub mount that allows a tumbling motion of the whole rotor. The study has been conducted in vertically sheared inflow under rated conditions. The time series of the deflection is extracted from the MBS-BEM results and added as prescribed motion to the CFD simulation. A significant reduction of the aerodynamic rotor bending moments (pitch and yaw) can be observed in the results of the CFD simulation, while aerodynamic rotor thrust and torque are almost not influenced. The fluctuations of the blade loads are also reduced. The 1P amplitude of the blade thrust force is reduced by more than 60% and the maximum is shifted towards 240° azimuth. This can be explained by a change of local AoA induced by the tumbling motion of the rotor. The comparison of BEM results and CFD results shows, that apart from small differences the loads as well as the load reduction can be captured adequately with the BEM approach. General differences can be explained as influence of the polars used in the BEM simulation. As the effects cannot be separated, it cannot be validated whether the influence of the tumbling motion of the rotor on the blade thrust force is considered correctly in the BEM approach.

Several simplifications have been made for the presented investigation. All structures have been considered as rigid except for the flexible hub and the tumbling motion of the rotor has been extracted from the MBS-BEM simulation and prescribed in the CFD simulation. The influence of the flexibility of other turbine components, especially the blades, as well as an interaction between CFD aerodynamics and structure have not been considered.

To overcome the limitations mentioned above, in a next step a Fluid-Structure-Coupling (FSC) approach using CFD for aerodynamics is intended, including blade elasticity as well as the hub degrees of freedom. This will allow more realistic investigations of the load reduction system and the suitability of the simplified approach used in this paper can be validated.

Nevertheless, the new load reduction system shows a high potential in reducing the pitching and yawing moments on the investigated two bladed wind turbine and potentially for two bladed wind turbines in general.

Acknowledgements

This project is founded by the German Federal Ministry for the Environment, Nature Conservation, Building and Nuclear Safety (BMUB). The simulations have been carried out at High Performance Computing Center Stuttgart (HLRS) funded by the Ministry of Science, Research and Arts and the Universities of the State of Baden-Württemberg, Germany, within the framework program bwHPC.

References

[1] Schorbach V and Dalhoff P 2012 *Proceedings of the EWEA Conference*
[2] Luhmann B, Cheng PW, Seyedin H 2014 *J. Phys.: Conf. Ser.* **524** 012049
[3] Luhmann B, Seyedin H, and Cheng PW 2015 *Proceedings of the DEWEK*
[4] Kroll N, Rossow C C, Becker K and Thiele F 2000 Aerospace Science and Technology 4 223–237
[5] Schulz C, Klein L, Weihing P, Lutz T and Krämer E 2014 *J. Phys.: Conf. Ser.* **524** 012134
[6] Weihing P, Meister K, Schulz C, Lutz T and Krämer E 2014 *J. Phys.: Conf. Ser.* **524** 012143
[7] Schulz C, Fischer A, Weihing P, Lutz T and Krämer E 2015 *High Performance Computing in Science and Engineering* (Springer International Publishing)
[8] Benek J, Steger J L and Dougherty F C 1983 AIAA Paper 83-1944
[9] Celik IB., Ghia U, and Roache PJ 2008 *Journal of fluids Engineering-Transactions of the ASME* 130.7
[10] Klein L, Lutz T and Krämer E 2014 *Proceedings of the 10th EAWE Phd Seminar in Europe*